THE MECHANISMS OF PHOTOREDOX SYSTEMS INVOLVING $Ru(bpy)_3^{2+}$, O_2 and Fe^{III}

W. JOHN ALBERY and ANDREW W. FOULDS†
Department of Chemistry, Imperial College, London SW7 2AY (Gt. Britain)
JAMES R. DARWENT‡
The Royal Institution, 21 Albemarle Street, London W1X 4BX (Gt. Britain)
(Received August 3, 1981)

Summary

The photoredox reactions between the couples $Ru(bpy)_3^{3+}$–$Ru(bpy)_3^{2+}$, Fe^{III}–Fe^{II} and O_2–H_2O_2–H_2O were studied using a variety of techniques which included measurements of the photostationary state, transients and nanosecond flash photolysis. Illumination of the O_2–$Ru(bpy)_3^{2+}$ system produces H_2O_2 from O_2 and H_2O by two separate photoredox systems, one involving $Ru(bpy)_3^{2+}$ and the other $Ru(bpy)_3^{3+}$. The mechanism of this system has been elucidated. In particular the rate constant for the electron transfer between caged $Ru(bpy)_3^{3+}$ and $O_2^{\cdot -}$ has been shown to be 10^9 s^{-1}. The complete mechanism for the network of significant reactions when ruthenium, iron and oxygen are all present was found. This system has been suggested as a possible photogalvanic cell. Studies of the photopotentials using a rotating disc electrode show that they are "mixed potentials" in which the electrode catalyses the oxidation of H_2O_2 by $Ru(bpy)_3^{3+}$; such measurements are no guide to the efficiency of possible photogalvanic systems.

1. Introduction

The Fe–Ru system has been suggested by Lin and Sutin [1] as a possible photoredox system for a photogalvanic cell designed to convert solar energy into electrical energy. An interesting feature claimed for this system is that the presence of oxygen makes very little difference to the photopotentials developed by the cell, provided that $[Fe^{III}]$ is large enough to react with most of the excited Ru^{II}. In this paper we examine the effect of oxygen on the photoredox system and the behaviour of the photopotentials.

†Present address: Shell Research Ltd., Thornton Research Centre, P.O. Box 1, Chester CH1 3SH, Gt. Britain.
‡Present address: Department of Chemistry, Birkbeck College, London WC1E 7HX, Gt. Britain.

0047-2670/82/0000-0000/$02.75

2. Experimental details

The kinetics of the photoredox systems were investigated by recording the absorbance of $Ru(bpy)_3^{2+}$ at $\lambda = 450$ nm when the cell was illuminated. In a typical experiment the absorbance was followed for about 200 s, at the end of which period a photostationary state was established. Details have been published elsewhere [2]; all experiments were carried out at 25 °C. The kinetics of the thermal reactions were followed on a Cary 14 spectrophotometer. Flash photolysis experiments were carried out using an Applied Photophysics KR-1 apparatus with a flash of $t_{1/2} \approx 10$ μs and on a Q-switched neodymium laser, frequency doubled through a CsH_2AsO_4 crystal, with a flash of $t_{1/2} \approx 15$ ns and a power of about 200 mJ. In both cases the change in the absorbance of Ru^{II} at $\lambda = 452$ nm was followed.

The photopotentials were measured first at a stationary platinum electrode in the photochemical cell and secondly at a rotating platinum disc electrode.

All chemicals were of AnalaR grade except for $Ru(bpy)_3^{2+}$ which was prepared by the method of Burstall [3]; solutions of $Ru(bpy)_3^{3+}$ were prepared either by oxidation with PbO_2 followed by centrifugation and filtration or by electrochemical oxidation at a platinum electrode. Air-saturated solutions were used to study systems involving O_2, and so the concentration of O_2 throughout was 0.3 mmol dm^{-3}. The standard concentration of $Ru^{II} + Ru^{III}$ was 20 μmol dm^{-3}. The medium for all experiments was 0.50 M H_2SO_4.

3. Results and discussion

Figures 1 and 2 show typical curves for the variation with time of $[Ru(bpy)_3^{3+}]$ calculated from the absorbance measurements for air-saturated solutions with no added Fe^{III}. The results in Fig. 1 show the approach to the photostationary state in the normal direction starting from Ru^{II} and in the

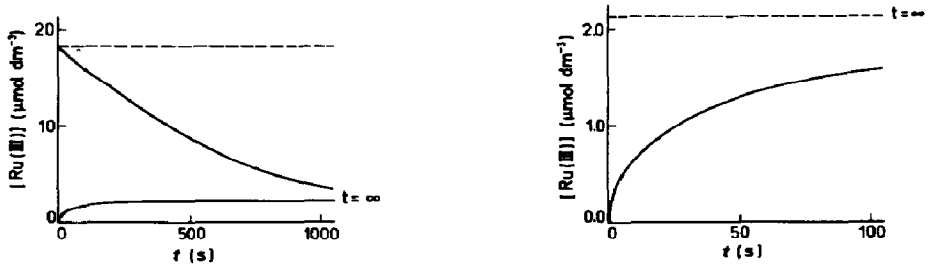

Fig. 1. Variation in $[Ru^{III}]$ with time in an air-saturated solution starting with either Ru^{II} or Ru^{III}: – – –, the rate of the thermal reaction of Ru^{III} with H_2O.

Fig. 2. The early part of the transient starting from Ru^{II} from Fig. 1: – – –, the photostationary state.

opposite direction where initially all the Ru^{II} has been oxidized to Ru^{III}. The same photostationary state is found regardless of the starting conditions. The broken line in Fig. 1 shows the rate of the thermal reaction of Ru^{III} with H_2O; it is much slower than the rate when the cell is illuminated. Spectrophotometric studies show that the first-order rate constant for the decomposition of $Ru(bpy)_3^{3+}$ in 0.5 M H_2SO_4 at 25 °C in the dark is approximately 2×10^{-5} s^{-1}, while the approach to the photostationary state in Fig. 1 takes only 200 s. This rate (starting from Ru^{III}) is not changed by the addition of Fe^{III} to the system. Furthermore the rate is not affected by the addition of H_2O_2 in concentrations up to 10^{-4} mol dm^{-3}.

We measured the second-order rate constant for the thermal reaction of Ru^{III} with H_2O_2 and found it to be 0.7 dm^3 mol^{-1} s^{-1}. Hence the concentration of H_2O_2 would have to be about 10^{-2} mol dm^{-3} before this thermal reaction could explain the behaviour shown in Fig. 1. We therefore conclude that the photochemical reaction is the oxidation of H_2O by Ru^{III}. The photostationary state that is observed is the balance between two photochemical reactions, one involving Ru^{II} and the other involving Ru^{III}. If photogenerated Ru^{III} were destroyed by a thermal reaction then the rate of this reaction would be so slow that nearly all the Ru^{II} would be converted to Ru^{III}.

We therefore consider the three photoredox and the 15 thermal one-electron transfer reactions displayed in Table 1 where for each pair of redox couples we have written the thermal reactions in the downhill direction. For the following reasons the seven thermal reactions in parentheses are insignificant and need not be further considered. First, of the four reactions in which $HO_2^{\cdot}$ and $OH^{\cdot}$ either react with each other or with themselves, because the concentration of $HO_2^{\cdot}$ is much larger than that of $OH^{\cdot}$ we need only consider the dismutation of $HO_2^{\cdot}$. Secondly the two reactions of $OH^{\cdot}$ with Fe^{II} and with Fe^{III} can be ruled out because the addition of Fe^{III} makes very little difference to the curve starting from Ru^{III} in Fig. 1. Thirdly for similar reasons the two reactions involving H_2O_2 can be ignored because

TABLE 1

The 18 possible electron transfer reactions

	Ru^{III}–Ru^{II}	O_2–$HO_2^{\cdot}$	$HO_2^{\cdot}$–H_2O_2	H_2O_2–$OH^{\cdot}$	$OH^{\cdot}$–H_2O
O_2–$HO_2^{\cdot}$	$Ru^{II*} + O_2 \rightarrow$ $Ru^{III} + HO_2^{\cdot} \rightarrow$				
$HO_2^{\cdot}$–H_2O_2	$Ru^{II} + HO_2^{\cdot} \rightarrow$	$HO_2^{\cdot} + HO_2^{\cdot} \rightarrow$			
H_2O_2–$OH^{\cdot}$	$Ru^{III} + OH^{\cdot} \rightarrow$	$(HO_2^{\cdot} + H_2O_2 \rightarrow O_2 + OH^{\cdot})$	$(HO_2^{\cdot} + OH^{\cdot} \rightarrow)$		
$OH^{\cdot}$–H_2O	$Ru^{III*} + H_2O \rightarrow$ $Ru^{II} + OH^{\cdot} \rightarrow$	$(OH^{\cdot} + HO_2^{\cdot} \rightarrow)$	$(H_2O_2 + OH^{\cdot} \rightarrow)$	$(OH^{\cdot} + OH^{\cdot} \rightarrow)$	
Fe^{III}–Fe^{II}	$Ru^{II*} + Fe^{III} \rightarrow$ $Ru^{III} + Fe^{II} \rightarrow$	$Fe^{III} + HO_2^{\cdot} \rightarrow$	$Fe^{II} + HO_2^{\cdot} \rightarrow$	$(Fe^{III} + OH^{\cdot} \rightarrow)$	$(Fe^{II} + OH^{\cdot} \rightarrow)$

the addition of modest amounts of H_2O_2 (about 10^{-4} M) does not affect the observed behaviour. We shall consider the remaining three photoredox and eight thermal reactions.

The reaction of Ru^{II*} with O_2 is complicated by the production of singlet oxygen [4, 5]. Winterle *et al.* [6] have studied a similar system to ours. They irradiated mixtures of $Ru(bpy)_3^{2+}$, O_2 and Fe^{II} and measured the production of Fe^{III}. They showed that the production of $HO_2^{\cdot}$ did not require the involvement of singlet oxygen. Our system differs from theirs in that we do not scavenge $HO_2^{\cdot}$ and Ru^{III} with added Fe^{II}, but like them we do not require the involvement of singlet oxygen.

With the reactions remaining in Table 1, the reaction scheme for the system with no added Fe^{III} is

Scheme 1

$$Ru^{II} + h\nu \xrightarrow{f_1} Ru^{II*}$$

$$Ru^{II*} + O_2 + H^+ \xrightarrow{\phi_1 f_1} Ru^{III} + HO_2^{\cdot}$$

$$HO_2^{\cdot} + Ru^{III} \xrightarrow{k_2} O_2 + Ru^{II} + H^+$$

$$HO_2^{\cdot} + Ru^{II} + H^+ \xrightarrow{k_3} H_2O_2 + Ru^{III}$$

$$HO_2^{\cdot} + HO_2^{\cdot} \xrightarrow{k_4} O_2 + H_2O_2$$

$$Ru^{III} + h\nu \xrightarrow{f_5} Ru^{III*}$$

$$Ru^{III*} + H_2O \xrightarrow{\phi_5 f_5} Ru^{II} + OH^{\cdot} + H^+$$

$$OH^{\cdot} + Ru^{II} + H^+ \xrightarrow{k_6} Ru^{III} + H_2O$$

$$OH^{\cdot} + Ru^{III} + H_2O \xrightarrow{k_7} H_2O_2 + Ru^{II} + H^+$$

By applying the steady state approximation to the intermediates of this scheme we find that

$$\frac{d[Ru^{III}]}{dt} = \frac{2k_4(\phi_1 f_1)^2}{(k_2[Ru^{III}] + k_3[Ru^{II}])^2} + \frac{2k_3[Ru^{II}]\phi_1 f_1}{k_2[Ru^{III}] + k_3[Ru^{II}]} - \frac{2k_7\phi_5 f_5[Ru^{III}]}{k_6[Ru^{II}] + k_7[Ru^{III}]} \quad (1)$$

On starting with Ru^{II}, the back reaction term in k_7 can be ignored for the first half of the reaction. The transient in Fig. 2 is sharply curved, and this curvature is caused by the $k_2[Ru^{III}]$ term dominating the denominators of

both the first two terms. At the start of the transient the percentage change in the concentration of Ru^{III} is considerable. However, on starting with Ru^{III} (Fig. 1) the transient is much less curved and this suggests that the denominator of the k_7 term is dominated by $k_7[Ru^{III}]$; at the start of the reaction in this direction there is no dramatic percentage change in $[Ru^{III}]$. Hence we simplify eqn. (1) by assuming

$$k_2[Ru^{III}] \gg k_3[Ru^{II}] \tag{2}$$

and

$$k_7[Ru^{III}] \gg k_6[Ru^{II}] \tag{3}$$

to obtain

$$\frac{d[Ru^{III}]}{dt} \approx \frac{2k_4(\phi_1 f_1)^2}{(k_2[Ru^{III}])^2} + \frac{2k_3[Ru^{II}]\phi_1 f_1}{k_2[Ru^{III}]} - 2\phi_5 f_5 \tag{4}$$

Depending on whether the photogeneration of Ru^{III} is described by the k_3 or the k_4 term, we find that the concentration of Ru^{III} and its dependence on f_1 and f_5 is given by

$$\log\left(\frac{[Ru^{III}]}{[Ru^{II}]}\right) = \frac{1}{2}\log\left(\frac{k_3\phi_1}{k_2\phi_5}\right) + \frac{1}{2}\log\left(\frac{f_1'}{f_5'}\right) \tag{5}$$

or

$$\log\left(\frac{[Ru^{III}]}{[Ru^{II}]}\right) = \frac{1}{3}\log\left(\frac{k_4\phi_1{}^2}{k_2{}^2\phi_5[Ru]_\Sigma}\right) + \frac{1}{3}\log\left(\frac{f_1{}^2}{f_5}\right) - \frac{1}{3}\log\left(\frac{[Ru^{II}]}{[Ru]_\Sigma}\right) \tag{6}$$

respectively where

$$f_1 = f_1'[Ru^{II}]$$

$$f_5 = f_5'[Ru^{III}]$$

$$[Ru]_\Sigma = [Ru^{II}] + [Ru^{III}]$$

Equation (5) predicts that for various neutral density filters of transmittance Φ the amount of photoconversion will be independent of Φ since the ratio f_1'/f_5' will not vary. In contrast, eqn. (6) predicts that, apart from the small correction term in Ru^{II}, the amount of conversion will depend on $\Phi^{1/3}$ since the ratio $f_1{}^2/f_5$ will be proportional to Φ. The results plotted in Fig. 3 show that eqn. (6) rather than eqn. (5) is obeyed; this implies that, in the photogeneration of Ru^{III} and H_2O_2 through f_1, the H_2O_2 is formed by the dismutation of $HO_2^{\cdot}$ (k_4) rather than by the reaction of $HO_2^{\cdot}$ with Ru^{II} (k_3). In Fig. 4 we depict the simplified reaction scheme deduced from the argument so far, together with some indication of the relative size of the fluxes through the different transition states.

We next discuss the transient behaviour. Starting with Ru^{III} we studied the system without oxygen so that there is no photogeneration of Ru^{III} and only the f_5 term is found in eqns. (1) and (4). Under these conditions the

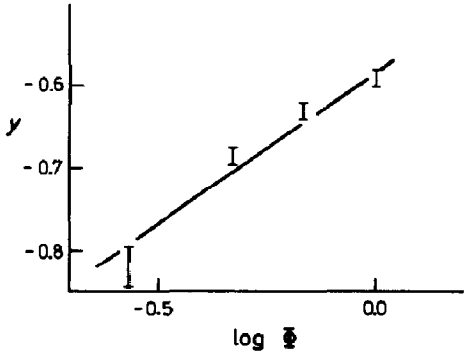

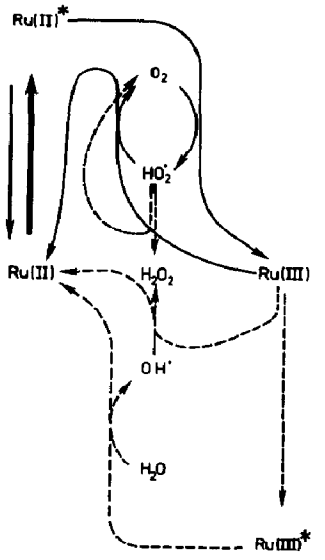

Fig. 3. Variation in the degree of conversion in the photostationary state with the transmittance Φ of various neutral density filters. The data are plotted according to eqn. (6) where $y = \log([Ru^{III}]/[Ru^{II}]) + \frac{1}{3}\log([Ru^{II}]/[Ru]_\Sigma)$.

Fig. 4. Reaction scheme for the Ru–O system. The widths of the arrows give some indication of the relative sizes of the different fluxes. In the photostationary state the net reaction of the whole system is $H_2O + \frac{1}{2}O_2 \rightarrow H_2O_2$.

transient obeys good first-order kinetics for at least three half-lives. The first-order rate constant was found to be proportional to the irradiance. This fact together with the shape of the transient confirms the simplified form of the f_5 term and the inequality in eqn. (3).

When the transient starts from Ru^{II} we rewrite eqn. (4), ignoring the k_3 terms, as

$$\frac{du}{dt} \approx 2\phi_5 f_5'\left(\frac{1}{u^2} - u\right) \tag{7}$$

where $u = [Ru^{III}]/[Ru^{III}]_{SS}$ and $[Ru^{III}]_{SS}$ is the concentration of Ru^{III} in the steady state. Equation (7) can be integrated to give

$$y = -\frac{1}{3}\ln(1 - u^3) = 2\phi_5 f_5' t \tag{8}$$

Figure 5 shows that the transient does indeed obey this equation. The value of $\phi_5 f_5'$ found from the gradient was in all cases in good agreement with the value from the first-order plot for the transient starting from Ru^{III}. The analysis of this transient therefore confirms the form of the k_4 term in eqn. (4) and the scheme in Fig. 4.

If the scheme is correct, then in a flash photolysis experiment Ru^{III} and $HO_2^{\cdot}$ will be generated. These species will then decay by the k_2 and k_4 reactions:

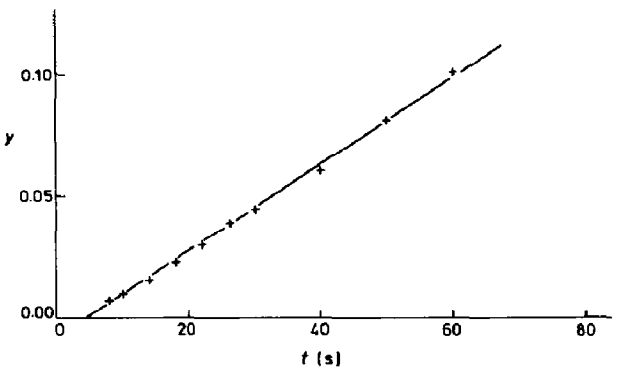

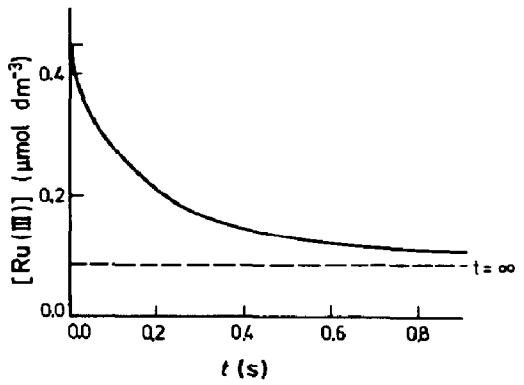

Fig. 5. Transient data from Fig. 1 (starting from Ru^{II}) plotted according to eqn. (8) where $y = -\frac{1}{3}\ln\{1 - ([Ru^{III}]/[Ru^{III}]_{SS})^3\}$.

Fig. 6. Decay of photogenerated Ru^{III} with time in a typical flash photolysis experiment. Because of the dismutation of $HO_2^{\cdot}$, residual Ru^{III} is left at the end.

$$HO_2^{\cdot} + Ru^{III} \xrightarrow{k_2} O_2 + Ru^{II} + H^+$$

$$HO_2^{\cdot} + HO_2^{\cdot} \xrightarrow{k_4} O_2 + H_2O_2$$

For every H_2O_2 molecule made there will be left behind two ions of Ru^{III}. Figure 6 shows typical results of a flash photolysis experiment and indeed residual Ru^{III} is formed. Taking the differential equations

$$da/dt = -k_2ab \tag{9}$$

$$db/dt = -k_2ab - 2k_4b^2 \tag{10}$$

where $a = [Ru^{III}]$ and $b = [HO_2^{\cdot}]$, dividing one into the other and integrating gives for the residual concentration a_∞ of the Ru^{III}

$$a_\infty/a_0 = \alpha^{1/(1-\alpha)} \tag{11}$$

where $\alpha = 2k_4/k_2$ and a_0 is the initial concentration of Ru^{III} which is equal to the initial concentration of $HO_2^{\cdot}$. We also obtain the general relation

$$b = \frac{a - \alpha a^{\alpha} a_0^{1-\alpha}}{1-\alpha}$$

Substitution in eqn. (9) followed by integration gives

$$B_\lambda(\alpha', 0) = B_\alpha(\alpha', 0) + k_2 a_\infty t \tag{12}$$

where

$$\alpha' = (1-\alpha)^{-1} \tag{13}$$

$$\lambda = (a_\infty/a)^{1/\alpha'} \tag{14}$$

and B is the incomplete beta function (ref. 7, p. 263).

From the residual concentration of Ru^{III}, we can find using eqn. (11) a value of α and using eqn. (13) a value of α'. By taking values of a during

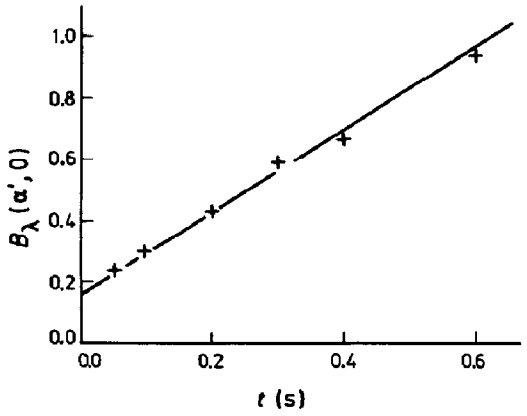

Fig. 7. Analysis of the data in Fig. 6 according to eqn. (12) where $B_\lambda(\alpha', 0)$ is the incomplete beta function.

the course of the reaction we can use eqn. (14) to find the appropriate value of λ; we then evaluate the incomplete beta function using the hypergeometric series (ref. 7, p. 556). Figure 7 shows a typical plot. A good straight line is obtained. From the gradient we find a value of k_2 and thence from α a value of k_4. The results are given in Table 2. The value for k_4 is in reasonable agreement with the value of 10^6 dm^3 mol^{-1} s^{-1} obtained by pulse radiolysis of formate solutions [8].

Flash photolysis was also used to measure the quantum efficiency ϕ_1 of the conversion of Ru^{II*} to Ru^{III}. By using a flash with $t_{1/2} \approx 15$ ns, the concentration of Ru^{II*} was measured before it had time to decay; ϕ_1 is then given by the ratio of the concentration of Ru^{III} at the start of the transient to the concentration of Ru^{II*}. We found

$$\phi_1 = (1.8 \pm 0.3) \times 10^{-2} \tag{15}$$

This value is in good agreement with that obtained by Winterle *et al.* [6] when allowance is made for the difference between oxygen-saturated and air-saturated solutions.

TABLE 2

Values of k_2 and k_4 from flash photolysis

k_2 (dm^3 mol^{-1} μs^{-1})	k_4 (dm^3 mol^{-1} μs^{-1})
15.4	2.3
10.7	2.0
12.3	2.4
11.8	1.8
12.5 ± 1.0	2.1 ± 0.1

TABLE 3

Interpretation of the kinetic parameters in schemes A, B and C

	ϕ_∞	ϕ_h (dm^3 mol^{-1})	ϕ_h/ϕ_∞ (dm^3 mol^{-1})	k_2 (dm^3 mol^{-1} μs^{-1})	k_{-D}' (ns^{-1})
Values	0.06	0.5	8	12.5	$< k_e, k_H[H^+]$
Scheme A	k_H/k_e''	k_H/k_e	k_e''/k_e	$k_D k_{-H}/k_{-D}$	$k_H[H^+]$
Scheme B	k_{-D}/k_e'	$k_H k_{-D}/k_e k_e'$	k_H/k_e	k_D	$k_e, k_H[H^+]$
Scheme C	k_{el}/k_{en}	$k_{el}k_H/k_{en}k_e$	k_H/k_e	$k_D k_e'/k_{-D}$	$k_e, k_H[H^+]$

There has been some controversy [5, 6] as to the interpretation of ϕ_1. A contributory factor to ϕ_1 is a Stern–Volmer quenching term:

$$Ru^{II*} \xrightarrow{k_T} Ru^{II}$$

$$Ru^{II*} + O_2 \xrightarrow{k_{O_2}}$$

where [9]

$$k_T = 1.67\ \mu s^{-1} \tag{16}$$

and

$$k_{O_2} = 3.3\ dm^3\ mol^{-1}\ ns^{-1} \tag{17}$$

giving for air-saturated solutions

$$\frac{k_{O_2}[O_2]}{k_T + k_{O_2}[O_2]} = \phi_{SV} = 0.37 \tag{18}$$

From eqn. (15) this leaves a factor $\phi_{O_2} \approx 0.049$. Winterle *et al.* [6] showed that

$$\phi_{O_2}^{-1} = \phi_\infty^{-1} + \phi_h^{-1}/[H^+] \tag{19}$$

where the values for ϕ_∞ and ϕ_h are as given in Table 3.

Three schemes can be suggested to interpret these results.

Scheme A

$$\begin{array}{ccc} & & \downarrow \phi_{SV} f_1 \\ Ru^{II} + {}^1O_2 & \xleftarrow{k_e} & (Ru^{III}, O_2^{\cdot -}) \\ Ru^{II} + {}^1O_2 + H^+ & \xleftarrow{k_e''[H^+]} & k_{-H} \uparrow\downarrow k_H[H^+] \\ & & (Ru^{III}, HO_2^{\cdot}) \underset{k_D}{\overset{k_{-D}}{\rightleftharpoons}} Ru^{III} + HO_2^{\cdot} \end{array}$$

Scheme B

$$\begin{array}{ccccc} & & \downarrow \phi_{SV} f_1 & & \\ Ru^{II} + {}^1O_2 & \xleftarrow{k_e} & (Ru^{III}, O_2^{\cdot -}) & & \\ & & \downarrow k_H[H^+] & & \\ Ru^{II} + {}^1O_2 + H^+ & \xleftarrow{k_e'} & (Ru^{III}, HO_2^{\cdot}) & \underset{k_D}{\overset{k_{-D}}{\rightleftharpoons}} & Ru^{III} + HO_2^{\cdot} \end{array}$$

Scheme C

$$\begin{array}{ccccc} & & \downarrow \phi_{SV} f_1 & & \\ Ru^{II} + {}^1O_2 & \xleftarrow{k_{en}} & (Ru^{II*}, O_2) & & \\ & & \downarrow k_{el} & & \\ Ru^{II} + {}^?O_2 & \xleftarrow{k_e} & (Ru^{III}, O_2^{\cdot -}) & \underset{k_D'}{\overset{k_{-D}'}{\rightleftharpoons}} & Ru^{III} + O_2^{\cdot -} \\ & & k_{-H} \uparrow \downarrow k_H[H^+] & & k_{-H'} \uparrow \downarrow k_{H'}[H^+] \\ Ru^{II} + {}^?O_2 + H^+ & \xleftarrow{k_e'} & (Ru^{III}, HO_2^{\cdot}) & \underset{k_D}{\overset{k_{-D}}{\rightleftharpoons}} & Ru^{III} + HO_2^{\cdot} \end{array}$$

The major product of the quenching by O_2 is singlet oxygen [4 - 6] shown as $^1O_2$. In scheme C because $^?O_2$ is formed by a minor route we cannot be certain whether it is singlet or triplet oxygen. In Table 3 we collect together the interpretation of the parameters in eqn. (19) and of k_2 according to the three different schemes. In scheme C we have also included an alternative route (shown by broken arrows) for the protonation of $(Ru^{III}, O_2^{\cdot -})$. Since $k_H'[H^+]$ is much greater than $k_D'[Ru^{III}]$, if $HO_2^{\cdot}$ were formed by this route ϕ_{O_2} would not vary with $[H^+]$ because the protonation would occur after the rate-limiting step (k_{-D}'). Hence we require for all schemes that k_{-D}' be smaller than the smallest first-order constant describing a route for the destruction of $(Ru^{III}, O_2^{\cdot -})$. These rate constants are listed in Table 3.

Scheme A is the original scheme proposed by Winterle *et al.* [6]. Scheme B is a variant of scheme A in which the protonation of $(Ru^{III}, O_2^{\cdot -})$ is followed by branching instead of the branching taking place in the protonation step. Scheme C is a version of a scheme suggested by Demas *et al.* [5] which has been modified to give the correct dependence on $[H^+]$.

From the results in Table 3 we can reject scheme B since it is unlikely that the diffusion-controlled rate constant k_D would be as low as the measured value of k_2 of 1.25×10^7 dm^3 mol^{-1} s^{-1}.

Turning to scheme A we note first that, if k_e'' is diffusion controlled, then k_H has to be an activated proton transfer and this is unlikely. Secondly the condition for k_{-D}' is rather improbable:

$$k_{-D}' < k_H[H^+] = 0.06 k_e''[H^+]$$
$$= 3 \times 10^8 \text{ s}^{-1} \quad (20)$$

where we have taken $k_e'' = 5 \times 10^{10}$ dm^3 mol^{-1} s^{-1} and $[H^+] = 0.1$ mol dm^{-3}. Thirdly the dissociation constant K_A for $HO_2^{\cdot}$ is 1.6×10^{-5} mol dm^{-3} [10]. With the value of k_H from eqn. (20) and $k_D \approx k_{-D}$ the calculated value of k_2 would be 5×10^4 dm^3 mol^{-1} s^{-1}, which is very much less than the observed value. Finally it is hard to see why the conversion through k_e'' should be catalysed by H^+, and, even if it is, how it can avoid the intermediate in scheme B. For all these reasons we reject scheme A.

In scheme C we take k_H to have a diffusion-controlled value of 5×10^{10} dm^3 mol^{-1} s^{-1}. This means that the condition for k_{-D}' for $[H^+] = 0.1$ mol dm^{-3} becomes

$$k_{-D}' \approx 5 \times 10^9 \text{ s}^{-1}$$

and this is possible for an ion pair. We then obtain

$$k_e \approx 6 \times 10^9 \text{ s}^{-1} \quad (21)$$

From the value of k_2 and taking $k_D \approx k_{-D}$ we find $k_e' \approx 10^7$ s^{-1}, and this means that the pK_A of the transition state for the electron transfer reaction between $HO_2^{\cdot}$ and Ru^{III} is between 2 and 3. This is consistent with our expectation that the pK_A of the transition state will be several units less than that for $HO_2^{\cdot}$. Thus a plausible interpretation of the data can be found using scheme C.

In eqn. (21) we have an estimate for the first-order rate constant for the fast electron transfer in the caged pair (Ru^{III}, $O_2^{\cdot -}$). From the standard electrode potentials for Ru^{III}–Ru^{II} [11] and for O_2–$O_2^{\cdot -}$ [12] we estimate that $\Delta G^{\ominus}$ for this reaction is -130 kJ mol^{-1}. The free energies of reorganization $\Delta G_{X,X}^{\ddagger}$ are 5 kJ mol^{-1} and 40 kJ mol^{-1} for the ruthenium [13] and the oxygen [14] couples respectively, giving a kinetic term $\Delta \bar{G}^{\ddagger}$ in the Marcus equation of 22 kJ mol^{-1} where

$$\Delta G_{X,Y}^{\ddagger} = \Delta \bar{G}^{\ddagger} + \alpha \Delta G^{\ominus} \quad (22)$$

with

$$\Delta \bar{G}^{\ddagger} = \tfrac{1}{2} (\Delta G_{X,X}^{\ddagger} + \Delta G_{Y,Y}^{\ddagger})$$

$$\alpha = \tfrac{1}{2} (1 + \Delta G^{\ominus}/4\Delta \bar{G}^{\ddagger})$$

For systems with such a small $\Delta \bar{G}^{\ddagger}$ and large negative $\Delta G^{\ominus}$, it has been suggested that the transition state may not lie between the minima of the intersecting Marcus parabolas. For this "inverse Marcus" system we estimate that the rate constant k_e would be as low as 10^{-3} s^{-1}. It is clear that the inverse Marcus model has to be rejected for the reaction between Ru^{III} and $O_2^{\cdot -}$ leading to ground state O_2.

It is possible that singlet oxygen is the product and this would mean that ΔG^{Φ} would be -40 kJ mol^{-1}. Using this value and the $\Delta G^{\ddagger}$ values given above we find from eqn. (22) that k_e would be 3×10^9 s^{-1} with $\alpha = 0.27$. This is consistent therefore with the observed value of k_e and a normal Marcus transfer.

We now return to eqn. (4) to discuss the concentration of Ru^{III} found in the steady state:

$$[Ru^{III}]_{SS} = k_4^{1/3}(\phi_1 f_1)^{2/3} k_2^{-2/3} (\phi_5 f_5')^{-1/3} \quad (23)$$

With $\phi_5 f_5' = 1.2 \times 10^{-3}$ s^{-1} measured from the transients, the only unknown on the right-hand side is f_1, and hence we find

$$f_1 = 5.4 \times 10^{-5} \text{ mol dm}^{-3} \text{ s}^{-1} \quad (24)$$

A check on this value, and indeed on the values of the other parameters, can be found by examining the early part of the transient. During this period the principal reactions are

$$\xrightarrow{\phi_1 f_1} Ru^{III} + HO_2^{\cdot} \xrightarrow{k_2}$$

and

$$HO_2^{\cdot} + HO_2^{\cdot} \xrightarrow{k_4}$$

Figure 8 shows concentration–time curves for Ru^{III} and $HO_2^{\cdot}$ calculated by computer simulation with $f_1 = 3.6 \times 10^{-5}$ mol dm^{-3} s^{-1} together with points from the early part of the Ru^{III} transient. Good agreement is found, again confirming the mechanism. It is interesting that the concentration of $HO_2^{\cdot}$ in the early stages matches that of Ru^{III} and only later falls away so that it can be treated by the steady state approximation.

Next we turn to experiments with $[Fe^{III}] = 2.0$ mmol dm^{-3} in which no oxygen was present. A typical concentration–time curve ($[O_2] = 0$) is shown in Fig. 9. The transient behaviour was too rapid to be observed in our apparatus. We consider the reactions in scheme 2.

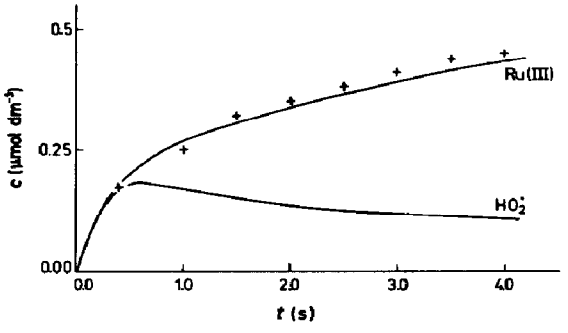

Fig. 8. Curves obtained from computer simulation for $[Ru^{III}]$ and $[HO_2^{\cdot}]$ in the early part of the transient; the data points are taken from Fig. 2.

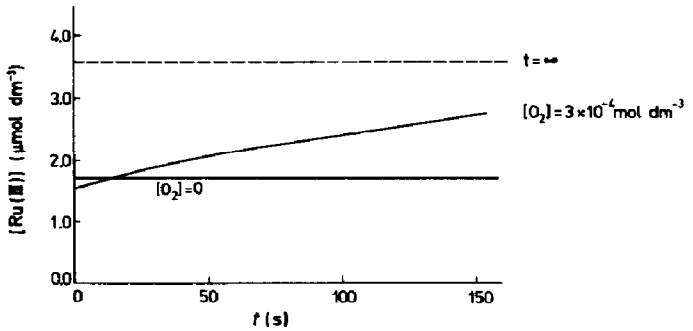

Fig. 9. Variation in $[Ru^{III}]$ with time in a solution with $[Fe^{III}] = 2$ mmol dm^{-3} and either $[O_2] = 0$ or $[O_2] = 0.3$ mmol dm^{-3}: – – –, the photostationary state in the presence of O_2.

Scheme 2

$$Ru^{II} \xrightarrow{f_1} Ru^{II*}$$

$$Ru^{II*} \xrightarrow{k_T} Ru^{II}$$

$$Ru^{II*} + Fe^{III} \xrightarrow{k_{Fe}} Ru^{III} + Fe^{II}$$

$$Ru^{III} + Fe^{II} \xrightarrow{k_8} Ru^{II} + Fe^{III}$$

If we assume that the reaction of Ru^{II*} with Fe^{III} to yield Ru^{III} has a quantum efficiency of unity [15, 16], the steady state concentration of Ru^{III} is given by

$$[Ru^{III}]_{ss,2} = \left\{ \frac{k_{Fe}[Fe^{III}]f_1}{(k_{Fe}[Fe^{III}] + k_T)k_8} \right\}^{1/2} \tag{25}$$

where $k_{Fe} = 2.7$ dm^3 mol^{-1} ns^{-1} [10] and $k_8 = 5.0$ dm^3 mol^{-1} μs^{-1} [10, 16]. From eqns. (23) and (25) we find that

$$\frac{[Ru^{III}]_{ss,2}}{[Ru^{III}]_{ss,1}} = \frac{B}{(1 + k_T/k_{Fe}[Fe^{III}])^{1/2}} \tag{26}$$

where

$$B = \frac{k_2^{2/3}(\phi_5 f_5')^{1/3}}{k_4^{1/3}\phi_1^{2/3}f_1^{1/6}k_8^{1/2}} \tag{27}$$

Using the experimental results for the ruthenium concentrations and eqn. (26) we find $B = 0.90$. A calculation of B from all the parameters in eqn. (27) with the values presented above gives $B = 1.50$. In view of the fact that this comparison involves results from nine different experiments, we consider that this agreement is reasonable.

By using neutral density filters, f_1 was varied and the dependence of $[Ru^{III}]_{SS}$ on f_1 was found to be approximately as $f_1^{1/2}$ as required by eqn. (25). Since $k_8[Ru^{III}]_{SS} \approx 10\ s^{-1}$, it is not surprising that the attainment of the steady state is too fast to be measured with our apparatus.

When both Fe^{III} and O_2 are present the concentration of Ru^{III} varies with time as shown in Fig. 9. At the start the oxygen makes little difference and $[Ru^{III}]$ rises rapidly to a value similar to that discussed for scheme 2. Subsequently the concentration increases over a similar period of time as that observed for scheme 1, but the final steady state concentration of 3.5 μmol dm^{-3} is *larger* than that for oxygen by itself (2.2 μmol dm^{-3}). The similar time scales arise because, as discussed above, the photochemical reaction of Ru^{III} with H_2O ($\phi_5 f_5$) is unaffected by the addition of Fe^{III}. However, the addition of Fe^{III} must reduce the flux that generates $HO_2^{\cdot}$ because Fe^{III}, present in a larger concentration, is more successful at capturing Ru^{II}* than O_2 is. Therefore to produce more Ru^{III} in the steady state, the photochemical reaction of Ru^{II} with O_2 must be assisted at some point by the presence of Fe^{III} or Fe^{II}. We suggest that, in addition to the k_4 reaction in scheme 1, H_2O_2 can be formed from $HO_2^{\cdot}$ by photogenerated Fe^{II}:

$$H^+ + HO_2^{\cdot} + Fe^{II} \xrightarrow{k_9} H_2O_2 + Fe^{III}$$

The complete reaction scheme is illustrated in Fig. 10. The concentration of Ru^{III} in the steady state is given by

$$[Ru^{III}]_{SS,3}{}^3 = \frac{f_1{}^2\phi_{O_2}k_{O_2}[O_2](\phi_{O_2}k_{O_2}[O_2]k_4/k_2 + k_9k_{Fe}[Fe^{III}]/k_8)}{k_2\phi_5 f_5'(k_{Fe}[Fe^{III}] + k_{O_2}[O_2] + k_T)^2} \quad (28)$$

Comparison with eqn. (23) shows that

$$r = \frac{[Ru^{III}]_{SS,3}}{[Ru^{III}]_{SS,1}} = \frac{(1 + k_2k_9k_{Fe}[Fe^{III}]/\phi_{O_2}k_{O_2}[O_2]k_4k_8)^{1/3}}{\{1 + k_{Fe}[Fe^{III}]/(k_{O_2}[O_2] + k_T)\}^{2/3}} \quad (29)$$

In this equation the only unknown is k_9. Figure 11 compares the experimental results with the curve calculated from eqn. (29) with

$$k_9 = 0.25\ dm^3\ mol^{-1}\ \mu s^{-1} \quad (30)$$

Very good agreement is found, confirming the addition of the k_9 reaction. It is interesting to note that because of the interplay of the k_9 route and the Stern–Volmer term the photogeneration of Ru^{III} exhibits a maximum and is therefore not very sensitive to $[Fe^{III}]$.

Furthermore we can rule out the involvement of the reaction of Fe^{III} with $HO_2^{\cdot}$:

$$Fe^{III} + HO_2^{\cdot} \xrightarrow{k_{10}} Fe^{II} + O_2 + H^+$$

From the measured ratio k_{10}/k_9 [17], which at our pH is about 10^{-3}, we find that

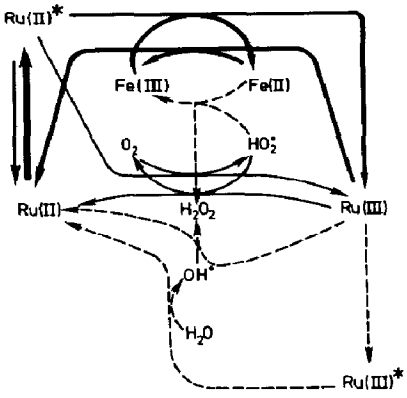

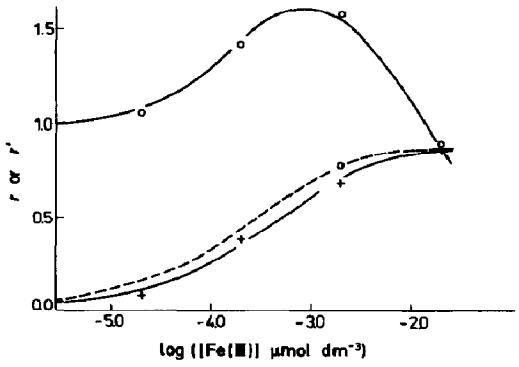

Fig. 10. Reaction scheme for the Fe–Ru–O system. Again the relative fluxes in the photostationary state are indicated by the widths of the arrows.

Fig. 11. Variation in r (○) and r' (+) with $[Fe^{III}]$ where r and r' are defined in eqn. (29) and eqn. (31) respectively: ———, $[O_2] = 3 \times 10^{-4}$ mol dm^{-3}; – – □ – –, $[O_2] = 0$.

$$\frac{k_{10}[Fe^{III}]}{k_2[Ru^{III}]} \approx 5[Fe^{III}] \text{ mol dm}^{-3}$$

Hence for $[Fe^{III}] < 2 \times 10^{-2}$ mol dm^{-3} the removal of $HO_2^{\cdot}$ by Fe^{III} is insignificant compared with its removal by Ru^{III}.

We can also describe the concentration of Ru^{III} formed in the initial rapid burst where the scheme 2 reactions predominate:

$$r' = \frac{[Ru^{III}]_{ss,2}}{[Ru^{III}]_{ss,1}} = \frac{B}{\{1 + (k_T + k_{O_2}[O_2])/k_{Fe}[Fe^{III}]\}^{1/2}} \qquad (31)$$

where B is defined in eqn. (27). This equation is the same as eqn. (26) with the addition of quenching by oxygen. In Fig. 11 we compare experimental results with a curve calculated from eqn. (31) with $B = 0.88$. Good agreement is found. We also show the curve for r' calculated with $[O_2] = 0$. The difference between this curve and the curve for r shows the effect that oxygen has on the generation of Ru^{III}. It can be seen that under our conditions for $[Fe^{III}] = 20$ mmol dm^{-3}, where the curves cross, the effect of O_2 on the observed $[Ru^{III}]_{ss}$ is nil, and indeed the experimental trace for this concentration shows no further increase in $[Ru^{III}]$ after the initial burst. The cross-over point depends on B and from eqn. (27) will be a function of the lamp spectrum and proportional to the irradiance to the power of one-sixth. In general, the addition of oxygen does change the steady state and in all cases it involves the reactions of scheme 1. It is interesting that, in the absence of O_2, although on a time scale of several seconds the concentration of Ru^{III} reaches the steady state value $[Ru^{III}]_{ss,2}$, this value cannot be maintained. The return of Ru^{III} to Ru^{II} by the photochemical back reaction means that the concentration of Ru^{III} should fall while the concentration of Fe^{II} should rise. However, in our apparatus the

fluxes were too small to be observed in comparison with the diffusion of O_2 into the cell and the slow photoaquation of Ru^{II} [18].

The final check that we carried out was to add a small amount of Fe^{II} to the system containing O_2 but no Fe^{III}. This causes an induction period while the added Fe^{II} is removed by the photogenerated $HO_2^{\cdot}$. The amount of Fe^{III} thereby generated is insignificant. Using scheme 1 together with the reaction signified by k_9 and the values of the parameters given above we calculated concentration–time curves by simulation with $f_1 = 4.2 \times 10^{-5}$ mol dm^{-3} s^{-1}. The results are compared with the experimental curve for [Ru^{III}] in Fig. 12. Good agreement is found confirming the value of k_9 deduced earlier.

Finally we turn to the question of the photopotentials generated by these systems. Typical results with a platinum electrode for the system with oxygen but no Fe^{III} are shown in Fig. 13. The potential developed by the electrode is some 100 mV less than the Nernst potential for the Ru^{III}–Ru^{II} couple. Like Lin and Sutin [1], we found that the potential was increased if the solution was stirred. Both of these facts suggest that we are observing a "mixed potential". From scheme 1 we suggest that the current from

$$Ru^{III} + e \rightarrow Ru^{II}$$

is exactly balanced by the current from

$$H_2O_2 \rightarrow O_2 + 2e + 2H^+$$

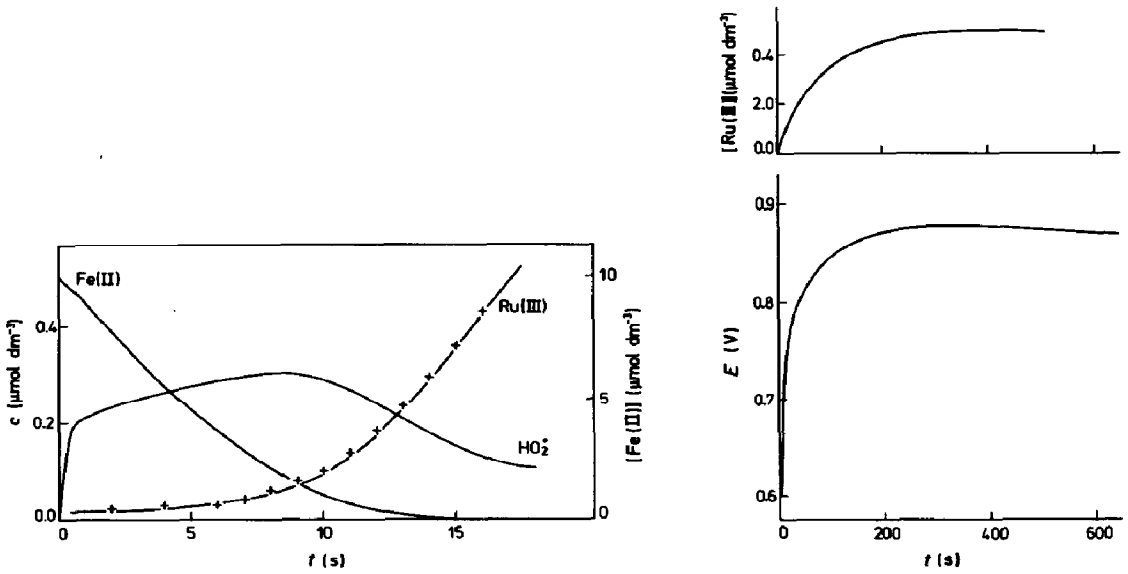

Fig. 12. Concentration–time curves obtained from computer simulation for the Ru–O system with added Fe^{II}: +, the observed variation in [Ru^{III}] with time.

Fig. 13. Typical variation with time of the photopotential at a stationary platinum electrode for the Ru–O system. The variation in [Ru^{III}] is also shown.

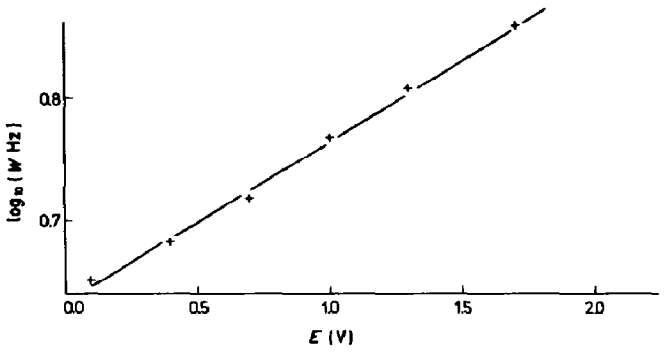

Fig. 14. Variation with the rotation speed W of the mixed potential at a rotating disc electrode for the Ru^{III}–H_2O_2 system, plotted according to eqn. (31).

This scheme explains why the photopotential goes through a maximum in Fig. 13. After $[Ru^{III}]$ reaches a steady state, the system is continuously generating H_2O_2 and so the potential shifts to more negative values.

Because Ru^{III} and H_2O_2 react so slowly we can investigate this system in the dark on a rotating disc electrode. Figure 14 shows results for the potential developed by a system containing $[Ru^{III}] = [H_2O_2] = 10$ μmol dm^{-3} and $[Ru^{II}] = 20$ μmol dm^{-3} as a function of the rotation speed. The potential is such that the current from Ru^{III} is close to its limiting current. The limiting current from H_2O_2 would be some five times greater because it is a two-electron system and because its diffusion coefficient is 3.5 times as large [19]. Using the Levich equation [20] and the usual treatment we find that

$$\frac{\alpha EF}{RT} = \text{constant} + \frac{1}{2} \ln W \tag{32}$$

where α is the transfer coefficient for the reduction of H_2O_2 and W is the rotation speed in hertz. From the good straight line in Fig. 14 we find $\alpha = 0.22$. The potential developed on a rotating disc electrode in an illuminated Ru^{II}–O_2 system gave similar behaviour with $\alpha = 0.25$. The photopotentials therefore confirm the production of H_2O_2. Similar qualitative behaviour was found when iron was present in the system. The fact that the photopotential is a mixed potential and therefore its size depends on the rate of supply of reactants to the electrode by mass transfer means that it is difficult to interpret and so is useless as a guide to the performance of this type of system in a photogalvanic cell. For this purpose full current–voltage curves have to be obtained [21] using a technique such as the transparent rotating disc electrode [22 - 24].

Acknowledgments

We thank the Science Research Council for financial support and Dr. William Beck for an interesting discussion on the incomplete beta function. This is a contribution from the Oxford–Imperial Energy Group.

References

1 C.-T. Lin and N. Sutin, *J. Phys. Chem., 80* (1976) 97.
2 W. J. Albery, W. R. Bowen, M. D. Archer and M. I. C. Ferreira, *J. Photochem., 11* (1979) 27.
3 F. H. Burstall, *J. Chem. Soc.*, (1936) 173.
4 J. N. Demas, D. Diemente and E. W. Harris, *J. Am. Chem. Soc., 95* (1973) 6864.
5 J. N. Demas, E. W. Harris and R. P. McBride, *J. Am. Chem. Soc., 99* (1977) 3547.
6 J. S. Winterle, D. S. Kliger and G. S. Hammond, *J. Am. Chem. Soc., 98* (1976) 3719.
7 M. Abramovitz and I. A. Stegun (eds.), *Handbook of Mathematical Functions*, Dover, New York, 1965.
8 D. Behar, G. Czapski, J. Rabani, L. M. Dorfman and H. A. Schwarz, *J. Phys. Chem., 74* (1970) 3209.
9 C.-T. Lin, W. Böttcher, M. Chou, C. Creutz and N. Sutin, *J. Am. Chem. Soc., 98* (1976) 6536.
10 E. Lee-Ruff, *Chem. Soc. Rev., 6* (1977) 195.
11 T. J. Meyer, *Acc. Chem. Res., 11* (1978) 94.
12 P. M. Wood, *FEBS Lett., 44* (1974) 22.
13 R. A. Marcus and N. Sutin, *Inorg. Chem., 14* (1975) 213.
14 J. Chevalet, F. Rouelle, L. Gierst and J. P. Lambert, *J. Electroanal. Chem., 39* (1972) 201.
15 D. G. Taylor and J. N. Demas, *J. Chem. Phys., 71* (1979) 1032.
16 W. J. Albery, W. R. Bowen, F. S. Fisher and A. D. Turner, *J. Electroanal. Chem., 107* (1980) 11.
17 C. Walling and M. Cleary, *Int. J. Chem. Kinet., 9* (1977) 595.
18 J. Van Houten and R. J. Watts, *Inorg. Chem., 17* (1978) 3381.
19 O. K. Borggaard, *Acta Chem. Scand., 26* (1972) 3393.
20 V. Levich, *Physicochemical Hydrodynamics*, Prentice Hall, Englewood Cliffs, NJ, 1962.
21 W. J. Albery and M. D. Archer, *J. Electrochem. Soc., 124* (1977) 688.
22 W. J. Albery, M. D. Archer, N. J. Field and A. D. Turner, *Discuss. Faraday Soc., 56* (1973) 28.
23 W. J. Albery, M. D. Archer and R. G. Egdell, *J. Electroanal. Chem., 82* (1977) 199.
24 W. J. Albery, P. N. Bartlett, W. R. Bowen, F. S. Fisher and A. W. Foulds, *J. Electroanal. Chem., 107* (1980) 23.